ISSN 2411-3336; e-ISSN 2541-9404

JOURNAL OF MINING INSTITUTE

Zapiski Gornogo instituta

Journal homepage: pmi.spmi.ru

Research article

Microstructural features of chromitites and ultramafic rocks of the Almaz-Zhemchuzhina deposit (Kempirsai massif, Kazakhstan) according to electron backscatter diffraction (EBSD) studies

Dmitrii E. Saveliev[1]✉, **Semen N. Sergeev**[2], **Darkhan K. Makatov**[3]

[1] *Institute of Geology, Ufa Federal Research Centre of the RAS, Ufa, Russia*

[2] *Institute for Metals Superplasticity Problems of the RAS, Ufa, Russia*

[3] *Abylkas Saginov Karaganda Technical University, Karaganda, Republic of Kazakhstan*

How to cite this article: Saveliev D.E., Sergeev S.N., Makatov D.K. Microstructural features of chromitites and ultramafic rocks of the Almaz-Zhemchuzhina deposit (Kempirsai massif, Kazakhstan) according to electron backscatter diffraction (EBSD) studies. Journal of Mining Institute. 2024. Vol. 266, p. 218-230.

Abstract. Microstructural features of the main rock-forming minerals of host ultramafic rocks (olivine, orthopyroxene) and chrome spinel from ores of the Almaz-Zhemchuzhina deposit were studied using the electron backscatter diffraction method. For ultramafic rocks, statistical diagrams of the crystallographic orientation of olivine and orthopyroxene were obtained, indicating the formation of a mineral association in conditions of high-temperature subsolidus plastic flow in the upper mantle. The main mechanisms were translation gliding and syntectonic recrystallization. Olivine deformation occurred predominantly along the (010)[100] and (001)[100] systems. The textural and structural features of chromitites reflect plastic flow processes, most pronounced in lenticular-banded ores. Microstructure maps in inverse pole figure encoding show differences in the grain size composition of the ores: areas consisting of disseminated chromitites are characterized by a finer-grained structure compared to lens-shaped segregations of a massive structure. Analysis of microstructure maps shows that during the transition from disseminated to massive ores, there is a widespread development of recrystallization, adaptation of neighbouring grains to each other, resulting in homogenization of crystallographic orientation in aggregates. The data obtained develop ideas about the rheomorphic nature of chromitite segregations in ophiolite dunites. It is assumed that the coarsening of the structure of massive chromitites is critically associated with an increase in the concentration of ore grains during solid-phase segregation within a plastic flow, when individual chrome spinel grains, initially separated by silicate material, begin to come into direct contact with each other.

***Keywords*:** ophiolites; chromitites; olivine; plastic deformation; EBSD; Kempirsai

Acknowledgments. The work was supported by the Russian Science Foundation grant N 22-17-00019. The research was carried out at the Collaborative Access Centre “Structural, Physical, and Mechanical Research of Materials” (IPSM RAS).

Received: 27.02.2023 ***Accepted: 25.10.2023*** ***Online: 08.02.2024*** ***Published: 25.04.2024***

Introduction. Ultramafic rocks of the Kempirsai massif in the Aktobe region of the Republic of Kazakhstan are associated with the largest reserves of ophiolite-type chromitites, “podiform deposits” [1-3], which differ from stratiform deposits by a sharp variability of morphological features and a constant association with extremely depleted mantle dunites. The specific morphology of deposits, sharp morphostructural variability, constant association with dunites and the absence of obvious signs of magmatic formation contributed to the emergence of various models of the origin of deposits of this type. To interpret the genesis of podiform deposits over the long history of their study, various models have been proposed with a predominant role of both magmatic and metasomatic processes. In recent decades, the reaction-magmatic [4-6] and fluid-metasomatic hypotheses [7, 8] have become the most widespread. Some works suggest the leading role of solid phase differentiation [9].

It is difficult to imagine the construction of full-fledged dynamic formation models of podiform chromitites without the use of quantitative data on their structure at various scale levels. Until the beginning of the 21st century and the advent of electron backscatter diffraction (EBSD) methods, this was practically impossible. Microstructural studies were limited to the study of transparent anisotropic host rock minerals, olivine and pyroxenes, using the Fedorov method [10-12].

Widespread use of electron microscopy with EBSD detectors since the beginning of the 21st century made it possible to obtain quantitative information about the internal structure of optically isotropic and non-transparent materials, including minerals of the cubic system [13-15] and various ore minerals [16-18]. In recent years, this research method has become widely used to assess the role of plastic deformations in mantle associations [19-21] and determine seismic anisotropy in the upper mantle of various regions based on the microstructure features of ultramafic xenoliths in kimberlites and alkali basalts [22-24].

To clarify the formation conditions for chromitites at the Almaz-Zhemchuzhina deposit in the southeastern part of the Kempirsai massif, the authors studied the material, macro- and micro-structural features of chromitites and their host ultramafic rocks using electron backscatter diffraction (EBSD). The main objectives of the research were: obtaining statistical data on the crystallographic orientation of rock-forming silicates (olivine, orthopyroxene) of ultramafic rocks, comparing them with experimental data; determination of the mechanisms of plastic deformation and recrystallization of olivine and orthopyroxene; microstructural study of aggregates of chrome spinel grains, obtaining data on the real structure of ore grains; assessment of the role of deformation and recrystallization in the formation of chromitites. Preliminary results of studying the samples are partially presented in [25].

Methods. In the 2022 field season, the authors studied chromitite samples of various structural types from dumps and boreholes of the Almaz-Zhemchuzhina deposit (Fig.1), as well as the most recent samples of host dunites and lherzolites selected from the core of the deep horizons at this site (depth from 420 to 1100 m).

At the preliminary stage, optical and electron microscopy methods were used. A total of 50 samples of peridotites, dunites, and chromitites, selected both from borehole cores and from deposit dumps, were studied. The composition of minerals was determined using a Tescan Vega Compact scanning electron microscope with an Xplorer-15 Oxford Instruments energy-dispersive detector at the Institute of Geology, Ufa Federal Research Centre of the Russian Academy of Sciences. The spectra were processed automatically by the AzTec One software package using the TrueQ technique. The following settings were used during the scanning: accelerating voltage 20 kV, probe current 3 nA, spectrum accumulation time at a point 60 s in Point&ID mode, beam diameter about 3 μm.

Three samples of the most recent ultramafic rocks from the GT-HY-1 borehole and two samples of chromitites from the dump of the Almaz-Zhemchuzhina deposit were selected for microstructural studies. From them, preparations were made that were oriented relative to the macroscopic elements of texture, banding, foliation, and lineation. The microstructure study of the preparations was carried out using the electron backscatter diffraction (EBSD) method on a Tescan Mira microscope at the Institute for Metals Superplasticity Problems of the Russian Academy of Sciences. The surface of the preparations for EBSD analysis was prepared by two-stage polishing, first mechanically using diamond pastes, and then by finishing mechanical and chemical polishing using a suspension based on colloidal silicon oxide (to remove hardening).

The main method of microstructural studies in this work, EBSD, is based on local anisotropic electron scattering on a crystal lattice [26, 27], which makes it possible to obtain Kikuchi lines, which are compared with reference ones for the phases present in the sample, then converted into data on the crystallographic orientation at any point of the sample under study. The phases are automatically identified at each point, and the *X* and *Y* coordinates of these points are stored in memory. Modern devices are capable of high-speed scanning with steps from tenths to several tens of μm [28], as a result of which software (for example, Channel 5) makes it possible to construct various maps in Hough space with a resolution of 100 pixels.

Journal of Mining Institute. 2024. Vol. 266. P. 218-230

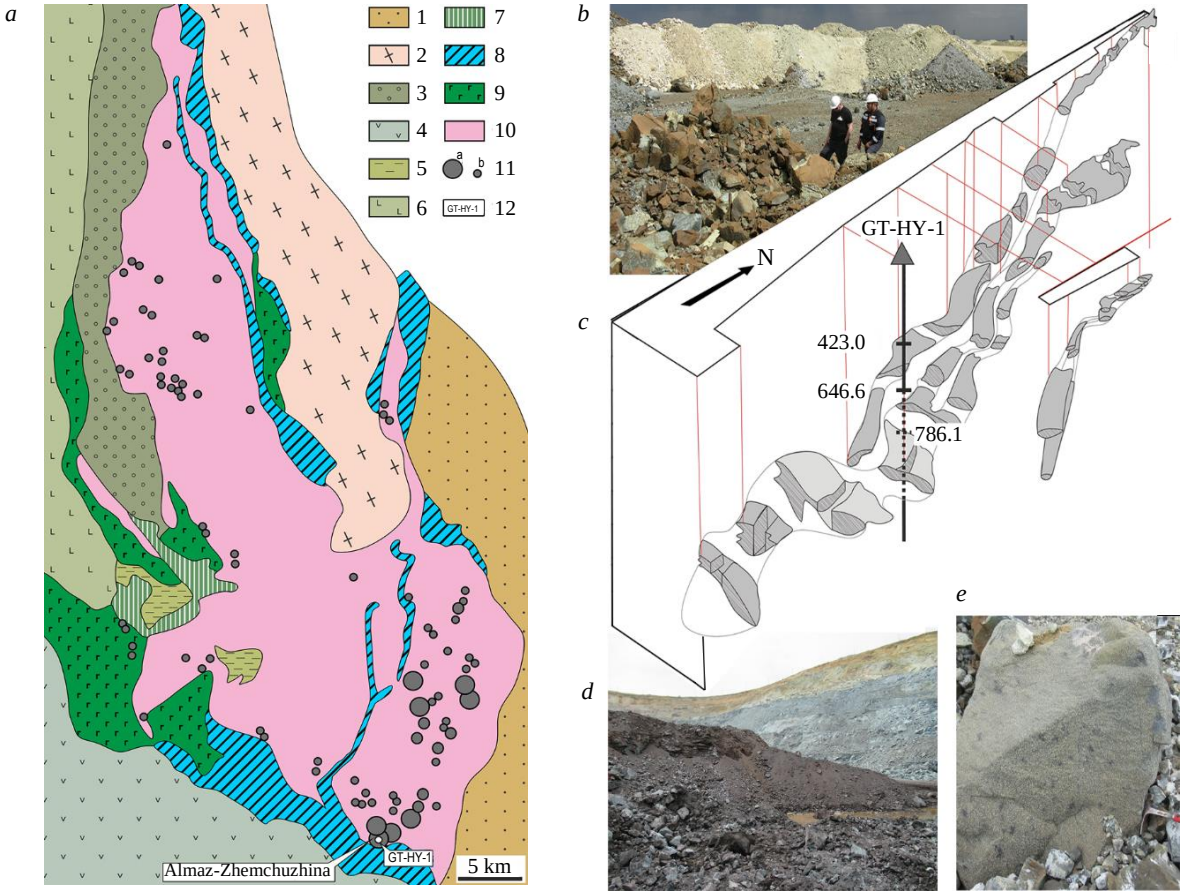

Fig.1. Geological position of the Almaz-Zhemchuzhina deposit and location of the studied samples:
a – small-scale map of the massif according to [34]; 1-6 – stratified rocks; 1 – South Mugodzhar zone (basalts (S-D_1, D_2), flyschoids and olistostromes (D_3-C_1); 2 – Ebety zone (basalt-andesite-rhyodacite, carbonate-silicite and greywacke formations (V?PZ_{1-2}); 3-6 – Sakmara zone (3 – basalt-andesite-dacite, greywacke, phtanite and carbonate formations (PZ_{1-2}), 4 – pillow lavas and pyroclastics of the basalt-andesite-rhyodacite formation with the participation of phtanites and clay-siliceous shales (PZ_{1-2}), 5 – phtanites and carbonate shales (O_2), 6 – pillow lavas of tholeiitic basalts with phtanite lenses (O_2); 7-10 – Kempirsai massif: 7 – sets of parallel diabase dikes and isotropic hornblende gabbros, 8 – Kyzylkain formation of pyroxenite-gabbro composition, 9 – Kokpekty formation of olivine gabbros and troctolites, 10 – rocks of the upper mantle section: harzburgites, lherzolites, dunites; 11 – chromitites (a – unique and large deposits; b – ordinary deposits and ore shows), 12 – location of studied boreholes and deposits; *b* – dumps of the Almaz-Zhemchuzhina deposit; *c* – block diagram of the ore cluster, including the Almaz-Zhemchuzhina, Millionnoe, and Pervomaiskoe deposits, location of the studied core samples; *d* – massive chromitites in the face of one of the open pits; *e* – sample of densely disseminated chromitite

In this work, EBSD scanning of preparations was carried out in steps of 10 to 20 μm with detail in some cases to 2 μm. In samples of serpentinized ultramafic rocks, predominantly texture diagrams were obtained, and in chromitites, it was possible to obtain fairly high-quality maps in inverse pole figure (IPF) encoding. A total of 25 areas were studied on seven preparations from five samples.

Research results. The Kempirsai massif is one of the largest ophiolite-type ultramafic massifs in the Urals, containing the world's largest deposits of chromium ores of this formation type. At the modern erosional truncation level, the massif is a pear-shaped body. It is elongated from north to south, according to the main direction of the Ural structures, and expands to the southeast (Fig.1). The massif is almost entirely composed of rocks of the so-called mantle section, harzburgites, lherzolites, and dunites, which near the surface are completely transformed into serpentinites. Due to the fact that serpentinization was limited to low-temperature facies with the formation of loop-shaped serpentine, the primary nature of serpentinites can be easily diagnosed by the presence of bastite pseudomorphs after pyroxenes. The most widespread in the massif are harzburgite serpentinites containing 70-80 vol.% olivine, 20-25 vol.% orthopyroxene, and a minor admixture of chrome spinel, which usually retains its composition.

In the southeastern part of the massif, along with homogeneous harzburgites, the dunite-harzburgite complex is widespread. Its structure is determined by the frequent alternation of harzburgite serpentinites and serpentinites without pseudomorphs after orthopyroxene (dunite). The most productive chromitite deposits of the massif are associated namely with the dunite-harzburgite complex.

In addition to ultramafic rocks, quite a lot of mafic dikes are found within the massif, among which gabbrodiabases of the Tygasha-Sai formation are the most widespread [29]. Rather large bodies of differentiated composition (Kokpekty complex) [29, 30], as well as tholeiitic basalts of the Sugraly complex and amphibolites [31] are developed in the near-contact parts of the massif. It should be noted that amphibolites cover the southern contact of the massif, under which the chromitite body of the largest deposit of the massif, Almaz-Zhemchuzhina, subducts.

When studying thin sections and polished sections using optical and electron microscopy, we found that the main minerals of the ores are high-chromium spinels (Cr/Cr + Al = 0.8-0.83) (Table 1), which is completely consistent with [1, 2], as well as serpentine and chlorite, replacing primary olivine. Chrome spinels contain mineral inclusions that are distributed very unevenly. The most common inclusion minerals are olivine (often serpentinized) and amphibole; less common are phlogopite, pyroxenes, and sulphides of basic metals (Fe, Ni, Cu, Co), as well as platinum group minerals [32, 33].

Table 1

Composition of ore-forming chrome spinels from the Almaz-Zhemchuzhina deposit

Oxide	Composition, wt.%*								
TiO_2	0.22	0.46	0.20	0.18	0.17	–	–	0.28	0.23
Al_2O_3	9.66	10.32	8.88	8.79	9.04	8.64	8.85	10.56	9.56
Cr_2O_3	62.16	61.97	63.18	62.64	62.56	63.13	63.64	61.03	62.47
Fe_2O_3**	2.1	0.24	3.48	2.37	2.94	3.23	3.12	2.11	1.34
FeO	13.13	13.1	11.1	12.3	11.85	11.33	12.5	12.2	12.4
MgO	13.39	13.28	14.92	13.72	14.33	14.42	14.09	14.00	13.77
NiO	–	–	–	–	0.18	0.24	–	0.20	–
Total	100.7	99.5	101.8	100.0	101.1	101.0	102.2	100.4	99.8
Element	Composition, apfu								
Al	0.367	0.395	0.332	0.336	0.341	0.326	0.331	0.398	0.364
Cr	1.582	1.590	1.582	1.606	1.580	1.599	1.597	1.545	1.597
Mg	0.642	0.642	0.704	0.663	0.682	0.688	0.666	0.668	0.663
Fe^{3+}	0.052	0.010	0.081	0.065	0.064	0.083	0.080	0.054	0.019
Fe^{2+}	0.352	0.351	0.297	0.325	0.324	0.298	0.325	0.322	0.351
Ti	0.005	0.011	0.005	0.004	0.004			0.007	0.006
Ni					0.005	0.006		0.005	
#Cr	0.81	0.80	0.83	0.83	0.82	0.83	0.83	0.79	0.81
#Mg	0.65	0.65	0.70	0.67	0.68	0.70	0.67	0.67	0.65

* SEM EDS data [33]; dash – contents below the detection limit.
** Contents are calculated based on the mineral stoichiometry.

Almost all ultramafic samples from borehole cores are characterized by clearly defined macroscopic structural elements – foliation (*S*) and lineation (*L*) (Fig.2, *a*, *b*). Foliation is due to the preferred orientation of tabular pyroxene grains in shape and to the aggregate banding often parallel to the same plane. Lineation is determined by the elongation of grains (pyroxene, olivine) or aggregates of chrome spinels in the plane of foliation. In chromitites, these macroscopic structural elements are most clearly manifested in samples of banded disseminated ores and in lenticular-banded ores, which we found in fairly copious quantities in the dumps of the Almaz-Zhemchuzhina deposit (Fig.2, *c*-*e*). Ores of this type most clearly show the participation in their formation of solid-phase plastic flow of mantle material. Samples of chromitites of this variety were used for microstructural studies.

Journal of Mining Institute. 2024. Vol. 266. P. 218-230

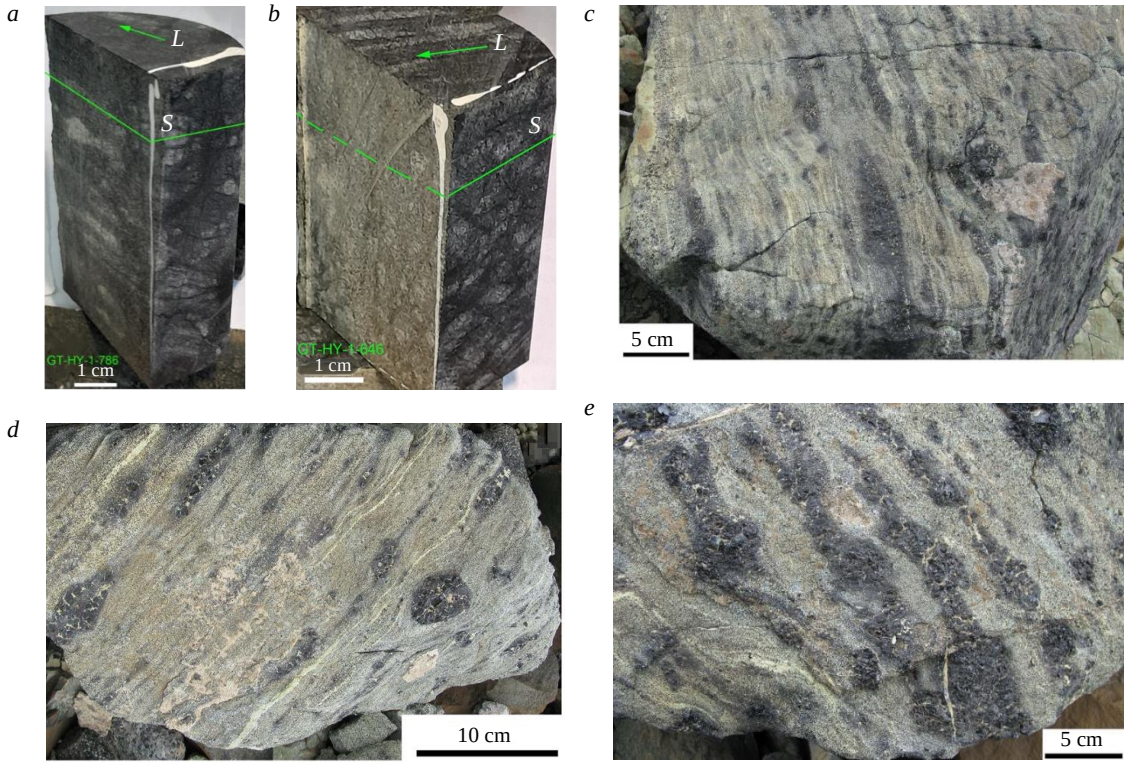

Fig.2. General view of the studied samples of host ultramafic rocks from deep borehole cores (*a*, *b*) and lenticular-banded chromitites from dumps (*c*-*e*)

Petrographic study of the host ultramafic rocks showed that dunites are significantly affected by serpentinization (at least 70 vol.%), while lherzolites contain areas with fairly good preservation (serpentine makes up less than 40 vol.% of the rock). The main rock-forming minerals of lherzolites show signs of high-temperature deformation: kink-band structures, undulose extinction (Fig.3, *a*), porphyroclastic structures caused by the association of deformed large orthopyroxene grains and zones of syntectonic recrystallization (RZ), composed of aggregates of small grains – neoblasts (Fig.3, *b*). Inside large deformed enstatite grains, the formation of diopside, amphibole lamellae and tiny chrome spinel grains is often observed (Fig.3, *c*). An idea of the typical mineralogical composition of lherzolites, the size and morphology of grains of rock-forming minerals is given by the EDS map in Fig.3, *d*.

The composition of the rock-forming minerals of ultramafic rocks is typical for rocks of the ophiolite mantle section: high-magnesium olivine; besides, from lherzolites to dunites the concentration of the forsterite minal increases from 90-92 to 95-96 %. Orthorhombic pyroxene is also represented by a high-magnesium variety, enstatite, and clinopyroxene by a calcium-magnesium variety, diopside. The composition of chrome spinels varies over a fairly significant range but is limited by isomorphism in the picotite-chromite series from 0.4 Cr# ($(Mg_{0.645}Fe_{0.355})_{1.00}(Al_{1.187}Cr_{0.759}Fe_{0.054})_{2.00}O_4$) in lherzolites to 0.8-0.85 ($(Mg_{0.704}Fe_{0.296})_{1.00}(Cr_{1.582}Al_{0.332}Fe_{0.081}Ti_{0.005})_{2.00}O_4$) in dunites and chromitites. In lherzolites, the permanent minor mineral is amphibole, the composition of which corresponds to calcium-magnesium varieties (pargasite-magnesian hornblende). In chromitites, olivine from inclusions in chrome spinel grains has the maximum magnesium composition (Fo_{97-98}) and abnormally high concentrations of nickel (to 1.8 wt.% NiO) (Table 2). According to the geothermometers [35-37], the closure of exchange reactions between olivine and chrome spinel occurred in the temperature range of 700-850 °C and oxygen fugacity from –1.04 to +2.8 ΔFMQ.

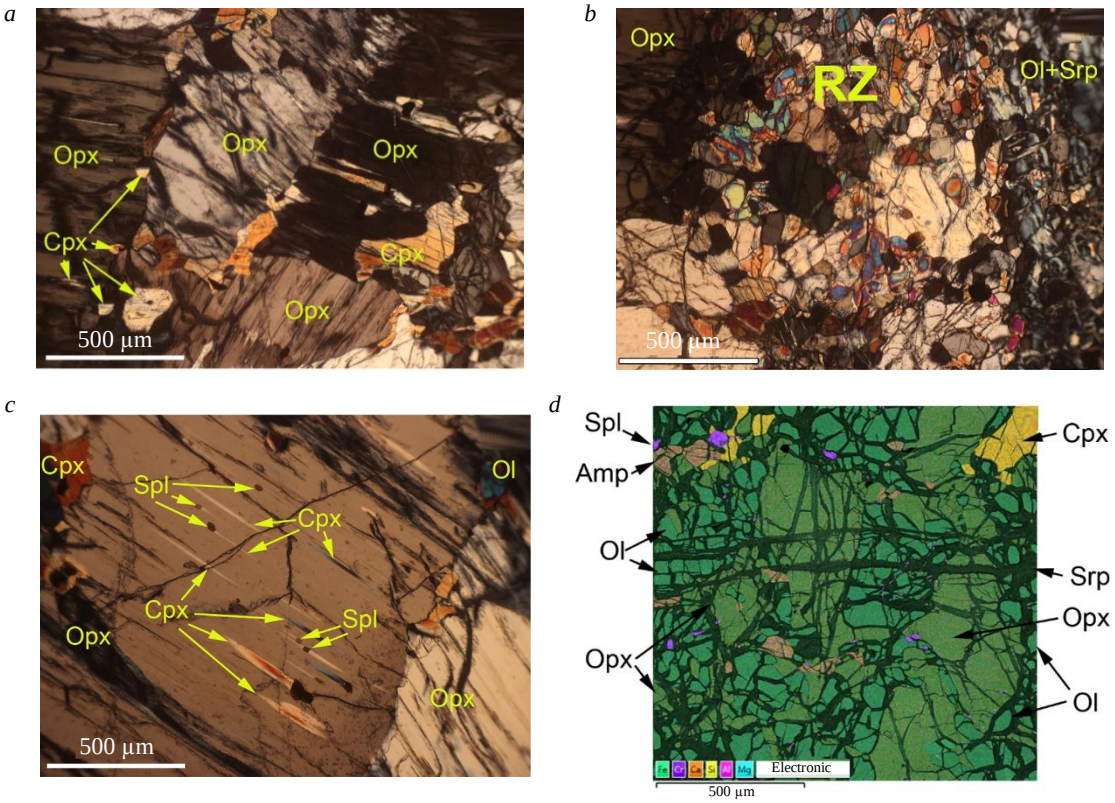

Fig.3. Petrographic features of ultramafic rocks from borehole GT-HY-1:
a – large deformed orthopyroxene grains with clinopyroxene inclusions;
b – recrystallization zone (RZ) composed of small newly formed grains (neoblasts) near a large deformed orthopyroxene grain;
c – isolation of new phases inside an orthopyroxene grain subject to plastic deformation;
d – typical EDS map of lherzolite from the ore-hosting strata of the Almaz-Zhemchuzhina deposit; Amp – amphibole;
Cpx – clinopyroxene; Ol – olivine; Opx – orthopyroxene; Spl – chrome spinel; Srp – serpentine

Table 2

Composition of olivine from inclusions in chrome spinels from the Almaz-Zhemchuzhina deposit

Oxide	Composition, wt.%								
SiO_2	41.30	41.31	41.38	41.11	40.61	41.50	41.10	42.56	42.75
FeO	2.77	2.94	1.87	2.12	2.45	2.58	2.62	2.97	2.51
MgO	54.71	55.38	55.06	54.47	53.84	56.05	54.78	54.94	55.26
NiO	0.65	0.69	1.66	1.83	1.51	0.95	0.94	1.41	0.67
Total	99.4	100.3	100.0	99.5	98.4	101.1	99.4	101.9	101.2
Element	Composition, apfu								
Si	0.982	0.973	0.978	0.978	0.978	0.969	0.977	0.993	1.000
Fe	0.055	0.058	0.037	0.042	0.049	0.050	0.052	0.058	0.049
Mg	1.951	1.956	1.953	1.944	1.944	1.963	1.953	1.923	1.939
Ni	0.012	0.013	0.032	0.035	0.029	0.018	0.018	0.027	0.013
Fo	0.973	0.971	0.981	0.979	0.975	0.975	0.974	0.971	0.975

Studying ultramafic samples using the EBSD method allowed us to obtain a series of texture diagrams (straight pole figures) for the main rock-forming minerals, olivine and orthopyroxene. Unfortunately, we did not manage to obtain complete microstructural maps due to significant serpentinization of the rocks, and in some cases due to the distorted crystal lattice of orthopyroxenes.

Textures obtained for olivine and orthopyroxene from host ultramafic rocks show a fairly strong preferred crystallographic orientation of both minerals. The following types of olivine textures are identified: 1) the maximum of the [100] axis near the foliation plane and near the lineation exposure, while the [001] axis forms a maximum on the flattening plane perpendicular to lineation, and the

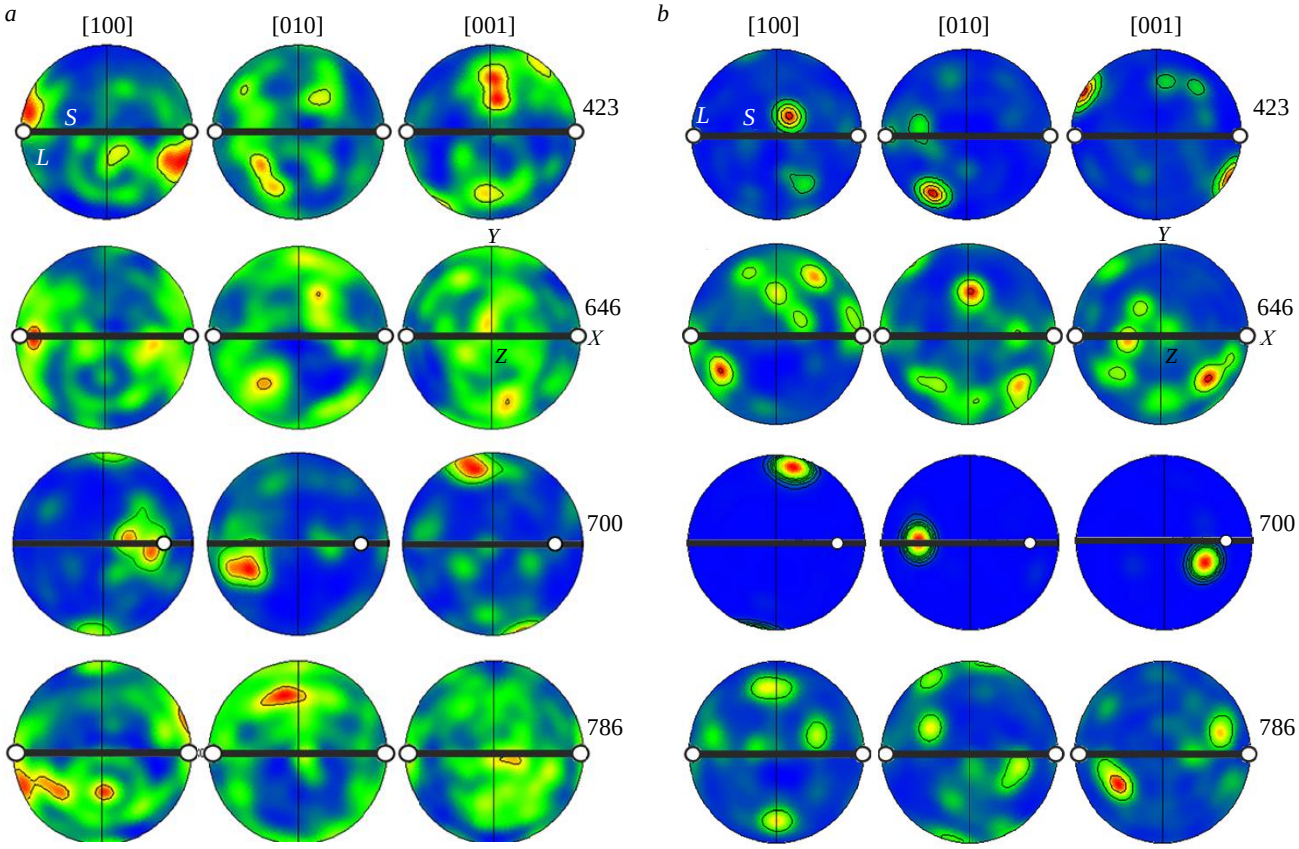

Fig.4. Straight pole figures for rock-forming olivine (*a*) and orthopyroxene (*b*)
from ultramafic rock samples from borehole GT-HY-1. Upper hemisphere of equal area projection;
S – projection of the plane of mineral flattening and banding; *L* – linearity exposures

maximum of the [010] axis is perpendicular to the flattening plane (samples 646, 786, Fig.4, *a*); 2) the maximum of the [100] axis is also near the flattening plane and the lineation exposure, but the other two axes change places: the [010] maximum is on the flattening plane, and the [001] maximum is perpendicular to it (sample 700, Fig.4, *a*).

In orthopyroxene, in almost all cases, coincidence or slight deviation of the [001] axis from the lineation exposure is registered (Fig.4, *b*), which indicates the direction of gliding. Glide planes in different samples are determined differently: (100) – in sample 700, (010) – in sample 423, and multiple planes in two other samples (Fig.4, *b*). Along with translation gliding, syntectonic recrystallization played a significant role in the studied ultramafic rock samples, which to some extent complicated the petrostructural patterns.

For microstructural studies, we selected a sample of densely disseminated chromitite with a lenticular-banded texture (Fig.5, *a*) with clearly defined macroscopic structural elements – banding and lineation, from which made preparations measuring 20×30 mm (Fig.5, *b*).

Macroscopic and mineragraphic study showed that the sample is a combination of sections with banded texture and medium-dense disseminated structure with the size of chrome spinel individuals 0.1-1 mm and chrome spinel aggregates of a massive lens-shaped structure with inclusions of silicate material. The size of individuals in massive aggregates is visually determined within 1-5 mm, however, it is not possible to determine the grain size more accurately due to the isotropic nature of the optical properties of chrome spinel (cubic system, opacity) and grain jointing (Fig.5, *c-e*). Microstructure studies using EBSD methods were carried out on preparation *c* (Fig.5, *b*), the scanning step was 20 μm in most areas, and one of them was studied in more detail with a step of 10 μm (Fig.5, *c-e*).

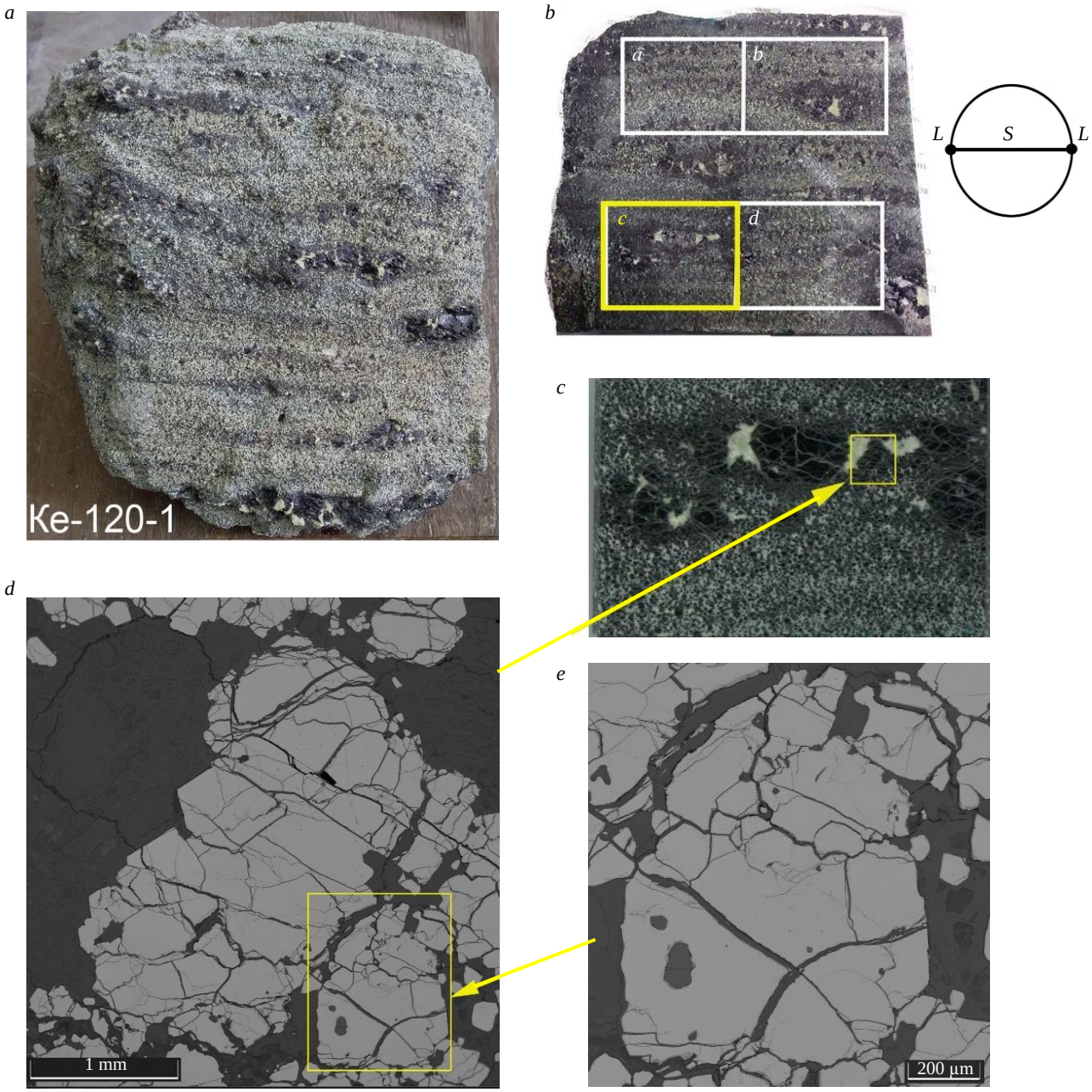

Fig.5. General view and structural details of the studied chromitite sample of lenticular-banded texture Ke-120-01: *a* – general view of the sample before preparation; *b* – view of part of the section perpendicular to the banding and macroscopic structural elements; *c* – general view of the preparation studied by the EBSD method; *d* – detail of the preparation with aggregates of a massive structure; *e* – one of the studied areas

The conducted instrumental microstructural studies generally confirmed the assumptions about the different grain size composition of sections with different textures (structures), which is most clearly manifested in maps compiled in colour-coded inverse pole figures (IPF) (Fig.6). The left part of Fig.6 shows the contrast maps of Kikuchi bands (KB), which characterize the quality of the measurements performed. In all the examples given, it is good, as evidenced by the uniform images and the predominance of light tones (sharp contrast of the KB). Darker areas indicate a greater degree of distortion in the crystal lattice of minerals. To understand the IPF maps, the inset (Fig.6, *h*) shows a typical colour key for the cubic system crystals.

In sections with disseminated structure, where chromite grains are separated from each other by a silicate matrix, most grains have a uniform orientation, the grain size is 70-250 μm (Fig.6, *a*, *b*).

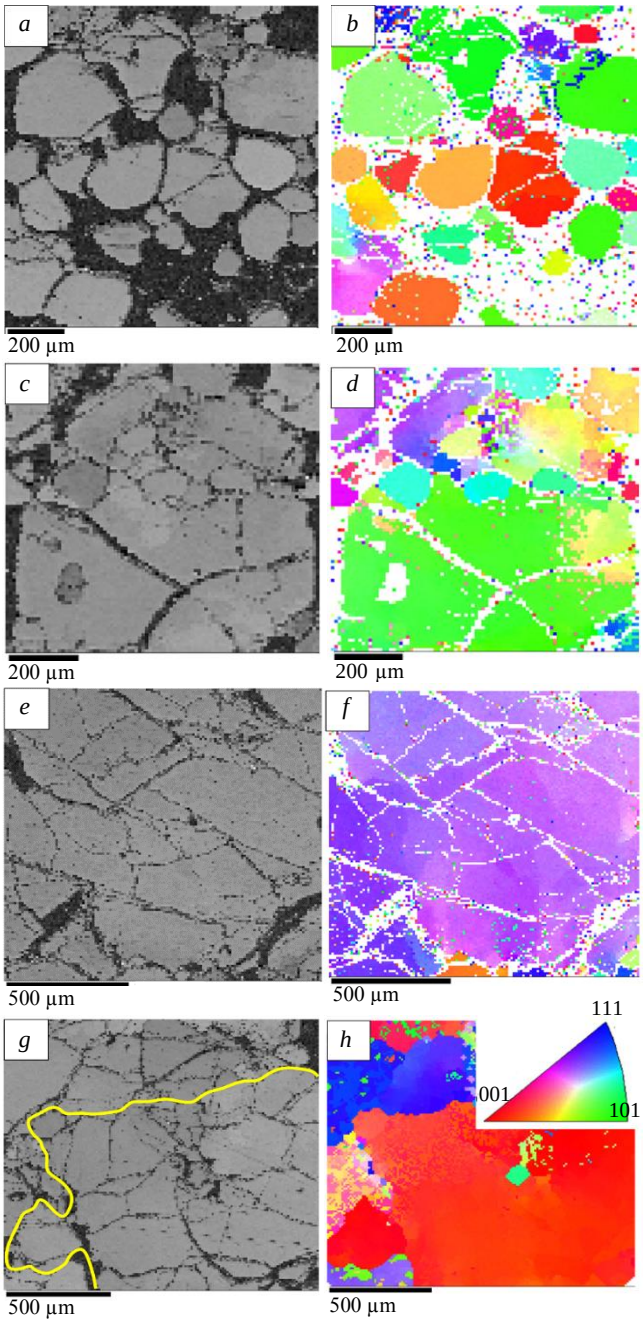

Fig.6. Microstructural maps of chromitite sample sections with lenticular-banded texture Ke-120-01:
a, *b* – section with disseminated structure (*a* – contrast of Kikuchi bands (KB), *b* – IPF map);
c, *d* – section with the transitional structure from disseminated to massive, shown in Fig.5, *e* (*c* – KB contrast, *d* – IPF map);
e-*h* – sections with massive structure (*e*, *g* – KB contrast, *f*, *h* – IPF maps); *g* – yellow colour shows the grain boundary with the {001} orientation on fragment *h*, in the inset – the colour key to the IPF maps

However, some grains exhibit a domain (subgrain) structure, the misorientation between subgrains is to 15°.

In transition-type chrome spinel aggregates (at the contact of the disseminated and massive zones) the presence of a heterogeneous structure with two maximum sizes of sections with uniform orientation is noted: 70-200 μm and over 500 μm (Fig.6, *c*, *d*). Within sections of the second type, one can often observe both local heterogeneities with low-angle boundaries of 1-10°, and small-sized inclusions separated from the matrix by high-angle boundaries (over 15°).

The internal parts of the sections with massive structure are areas with an almost uniform structure, the misorientation angle does not exceed 5° (Fig.6, *e*, *f*). The boundaries between blocks with homogeneous structure can be sharp and at the same time completely independent of the visually observed physical sections expressed by thin fractures (Fig.6, *g*, *h*).

In addition to studying the main rock-forming and ore-forming minerals of ultramafic rocks (olivine and orthopyroxene) and chromitites (chrome spinels) in the southern part of the Kempirsai massif, we investigated the internal structure of minerals rarer for ultramafic rocks, clinopyroxenes, which are represented by the calcium-magnesium variety, diopside ($CaMg(Si_2O_6)$). A noticeable presence of diopside is observed in three studied samples of partially serpentinized peridotites, 646, 700, and 786. The EBSD study revealed the presence of rather strong preferred crystallographic orientations of this mineral at index values M = 0.1-0.4 (Fig.7). It should be noted that only in sample 700 there is a coincidence between the maximum intensity of the exposures of one of the [001] axes with the lineation direction and the maximum of the [100] axis, perpendicular to the foliation plane, which is characteristic of the (100) [001] slip system. This slip system is also the most typical for orthopyroxenes. In the other two samples, more diffuse texture patterns were obtained, which may be due to two main reasons: a considerable proportion of recrystallized diopside grains in the studied samples, as well as the presence of crystals that have undergone melting (fragments of a crystallized partial melt).

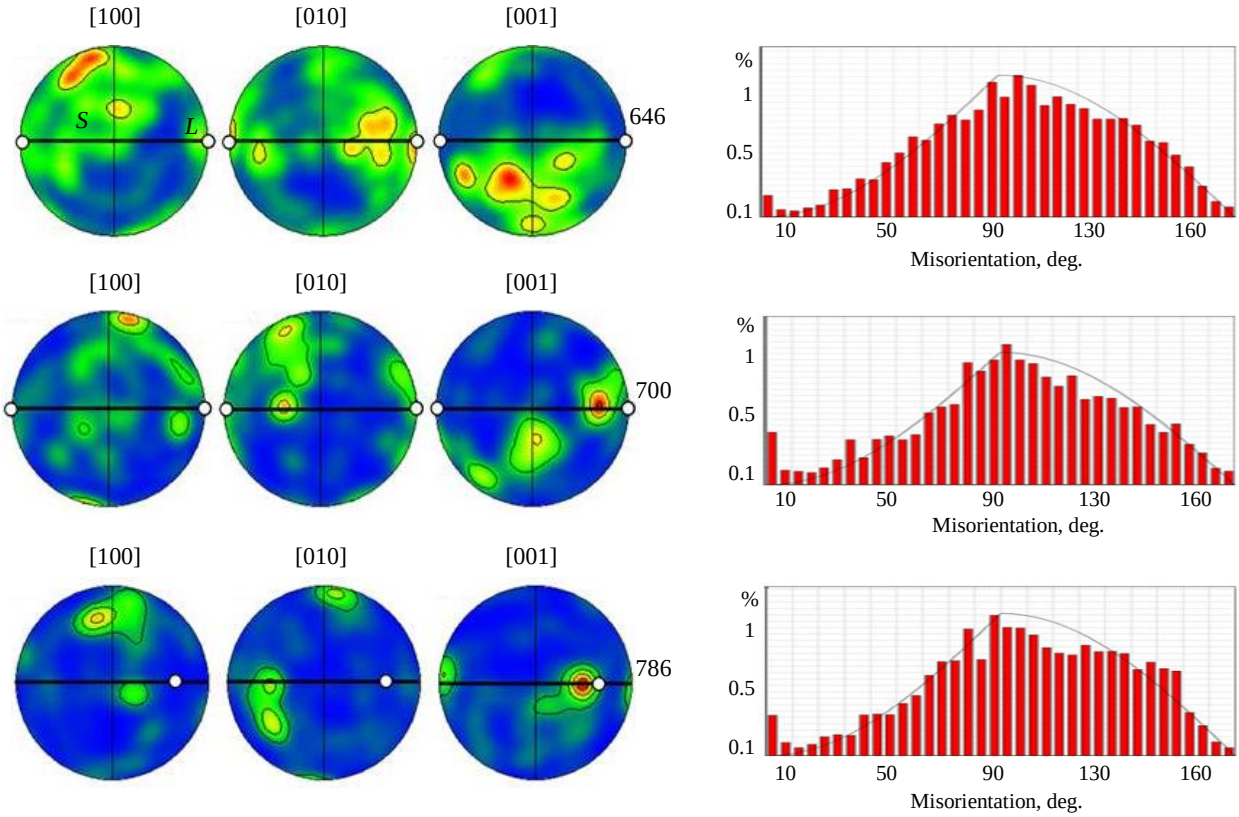

Fig.7. Straight pole figures for clinopyroxenes from ultramafic rock samples from borehole GT-HY-1

Discussion of the results. The obtained petrographic, mineralogical, and microstructural data are generally consistent with the overall structural patterns of ultramafic rock complexes and chromitite deposits [4], although in part they diverge from some well-known provisions. In the studied chromite-bearing section, lherzolites with aluminous spinel are quite widespread. Dunites contain high-chromium accessory chrome spinel, and olivine from inclusions is very enriched in nickel [32, 33]. All this indicates a high degree of depletion of wallrock ultramafic rocks, although in general the section is represented by relatively weakly depleted rocks of the upper mantle.

The obtained microstructural data indicate the formation of ultramafic rocks in the conditions of high-temperature plastic flow, accompanied by syntectonic recrystallization [25]. Judging by the texture diagrams, two slip systems (010)[100] and (001)[100] appeared in olivine, which correspond to texture types A and E according to the classification [38]. Both types of textures were diagnosed in experiments under stress to 300 MPa, type A being observed in “dry” (<200 ppm H/Si), and type E in “wet” conditions (200-1000 ppm H/Si) [38] .

More complex petrostructural patterns were obtained in orthopyroxene, which is associated with the lower plasticity of this mineral compared to olivine [39, 40] and, as a consequence, the presence of several groups of grains, deformed porphyroclasts with a domain structure and neoblasts formed during syntectonic recrystallization.

Macrotextural and microstructural features of chromitites were also formed in the conditions of plastic flow of host dunites with dispersed ore material. This is especially pronounced in lenticular-banded varieties of ores. Differences in the grain size composition of sections with disseminated and massive structure are well explained precisely from the position of the solid-phase genesis of ores. According to the rheomorphic model [9, 32, 41], the most mobile members of the mantle sections of ophiolites are dunites, formed as a result of the deformation-induced decomposition of orthopyroxenes [41]. The same process leads to a primary increase in the concentration of chrome spinels, which

crystallize from impurity amounts of chromium and aluminium included in pyroxenes. Since olivine is the mineral with the weakest rheological properties in the upper mantle [39], plastic flow and associated solid-phase differentiation of matter are localized in dunite zones. Due to a significantly higher rheological rigidity, chrome spinel grains in an olivine aggregate predominantly behave as rigid inclusions, which are energetically advantageous to form clusters – segregations – in such a solid-phase flow, as was shown by physical and mathematical modelling in [9].

Thus, inside the dunites, segregation of chromite grains could occur with the formation of lenticular-banded accumulations. In the central parts of the lenses, conditions were created for the contact of initially scattered ore grains. At their contacts, the initial misorientation was levelled, i.e. a new grain with a uniform crystallographic orientation was formed. A similar mechanism was proposed to explain the microstructure features in Indian chromitites [42] and is close to "high-P sintering", which is proposed to explain the genesis of coarse-grained massive chromitites in both ophiolitic and layered complexes [43, 44].

Microstructural studies confirmed the previously stated assumption that the sizes of chrome spinel individuals critically depend on structural features, and those, in turn, on the segregation stage. At the early stage, each chrome spinel grain is surrounded by olivine grains, therefore, the size of ore grains has one maximum, corresponding to deformation conditions and is always equal to or less than the size of olivine grains. However, when segregation reaches a certain critical level, which can be conventionally designated as "the beginning of grain contact," the growth of chromite aggregates (accretion) and the erasure of orientation differences begin. This direction of the process is facilitated by the significantly lower deformability of chromite compared to olivine and the slowdown of plastic flow near areas with increased concentration of ore grains. A similar mechanism for the growth of large grains (porphyroblasts) of minerals with stronger rheological properties (in particular, garnets) in metamorphic rocks was described in [45].

Conclusion. Microstructural studies of chromitites and host ultramafic rocks of the Almaz-Zhemchuzhina deposit allowed us to obtain quantitative data on the internal structure of the rocks. We found out that the formation of ultramafic rocks occurred in the conditions of subsolidus high-temperature (650-950 °C) plastic flow. Statistical data on the crystallographic orientation of olivine indicate that the main mechanism of deformation was translation gliding along the (010)[100] and (001)[100] systems; syntectonic recrystallization was of subordinate importance. In orthopyroxene, plastic flow was also realized by the mechanism of translation glide: systems (100)[001] and (010)[001], while syntectonic recrystallization was much stronger compared to olivine. Chromitites also exhibit textures and structures formed in plastic flow conditions. Disseminated ores have a finer-grained structure compared to massive ones: in the structure formation of the latter, the accretion of ore grains played a significant role, which was accompanied by the unification of their crystallographic orientation.

REFERENCES

1. Kravchenko G.G. The role of tectonics in the crystallization of chromite ores in the Kempirsai pluton. Moscow: Nauka, 1969, p. 217 (in Russian).

2. Pavlov N.V., Kravchenko G.G., Chuprynina I.I. Chromites of the Kempirsai pluton. Moscow: Nauka, 1968, p. 179 (in Russian).

3. Melcher F., Grum W., Simon G. et al. Petrogenesis of the Ophiolitic Giant Chromite Deposits of Kempirsai, Kazakhstan: a Study of Solid and Fluid Inclusions in Chromite. *Journal of Petrology*. 1997. Vol. 38. Iss. 10, p. 1419-1458. DOI: 10.1093/petroj/38.10.1419

4. González-Jiménez J.M., Griffin W.L., Proenza J.A. et al. Chromitites in ophiolites: How, where, when, why? Part II. The crystallization of chromitites. *Lithos*. 2014. Vol. 189, p. 140-158. DOI: 10.1016/j.lithos.2013.09.008

5. Yao Wu, Mengjing Xu, Zhenmin Jin et al. Experimental constraints on the formation of the Tibetan podiform chromitites. *Lithos*. 2016. Vol. 245, p. 109-117. DOI: 10.1016/j.lithos.2015.08.005

6. Fahui Xiong, Basem Zoheir, Richard Wirth et al. Mineralogical and isotopic peculiarities of high-Cr chromitites: Implications for a mantle convection genesis of the Bulqiza ophiolite. *Lithos*. 2021. Vol. 398-399. N 106305. DOI: 10.1016/j.lithos.2021.106305

7. Johan Z., Martin R.F., Ettler V. Fluids are bound to be involved in the formation of ophiolitic chromite deposits. *European Journal of Mineralogy*. 2017. Vol. 29. Iss. 4, p. 543-555. DOI: 10.1127/ejm/2017/0029-2648

8. Pushkarev E.V., Kamenetsky V.S., Morozova A.V. et al. Ontogeny of ore Cr-spinel and composition of inclusions as indicators of the pneumatolytic-hydrothermal origin of PGM-bearing chromitites from Kondyor massif, the Aldan Shield. *Geology of Ore Deposits.* 2015. Vol. 57. Iss. 5, p. 352-380. DOI: 10.1134/S1075701515050049

9. Saveliev D.E., Fedoseev V.B. Solid-state redistribution of mineral particles in the upwelling mantle flow as a mechanism of chromite concentration in the ophiolite ultramafic rocks (by the example of Kraka ophiolite, the Southern Urals). *Georesursy.* 2019. Vol. 21. N 1, p. 31-46 (in Russian). DOI: 10.18599/grs.2019.1.31-46

10. Kazakov A.N. Dynamic analysis of microstructural orientations of minerals. Leningrad: Nauka, 1987, p. 272 (in Russian).

11. Saranchina G.M., Kozhevnikov V.N. Fedorov method (determination of minerals, microstructural analysis). Leningrad: Nedra, 1985, p. 208 (in Russian).

12. Chernyshov A.I., Yurichev A.N. The Structural Evolution of Dunite and Chromite Ore from the Kharcheruz Massif, the Polar Urals. *Geotectonics.* 2016. Vol. 50. N 2, p. 62-77. DOI: 10.1134/S0016852116020035

13. Klepikov I.V., Vasilev E.A., Antonov A.V., Kudryavtsev A.A. Growth of pyramids {110} in natural diamonds. *Geology of Ore Deposits.* 2022. Vol. 64. Iss. 8, p. 670-675. DOI: 10.31857/S0869605521010068

14. Klepikov I.V., Vasilev E.A., Antonov A.V. Regeneration Growth as One of the Principal Stages of Diamond Crystallogenesis. *Minerals*. 2022. Vol. 12. Iss. 327. DOI: 10.3390/min12030327

15. Vasilev E.A., Kriulina G.Y., Garanin V.K. Thermal history of diamond from Arkhangelskaya and Karpinsky-I kimberlite pipes. *Journal of Mining Institute.* 2022. Vol. 255, p. 327-336. DOI: 10.31897/PMI.2022.57

16. Till J.L., Moskowitz B.M. Deformation microstructures and magnetite texture development in synthetic shear zones. *Tectonophysics*. 2014. Vol. 629, p. 211-223. DOI: 10.1016/j.tecto.2014.04.026

17. Vukmanovic Z., Barnes S.J., Reddy S.M. et al. Morphology and microstructure of chromite crystals in chromitites from the Merensky Reef (Bushveld Complex, South Africa). *Contributions to Mineralogy and Petrology*. 2013. Vol. 165. Iss. 6, p. 1031-1050. DOI: 10.1007/s00410-012-0846-1

18. Yudovskaya M.A., Costin G., Shilovskikh V.V. et al. Bushveld symplectic and sieve-textured chromite is a result of coupled dissolution-reprecipitation: a comparison with xenocrystic chromite reactions in arc basalt. *Contributions to Mineralogy and Petrology*. 2019. Vol. 174. Iss. 9. N 74. DOI: 10.1007/s00410-019-1613-3

19. Bernard R.E., Behr W.M., Becker T.W., Young D.J. Relationships Between Olivine CPO and Deformation Parameters in Naturally Deformed Rocks and Implications for Mantle Seismic Anisotropy. *Geochemistry, Geophysics, Geosystems*. 2019. Vol. 20. Iss. 7, p. 3469-3494. DOI: 10.1029/2019GC008289

20. Kumamoto K.M., Warren J.M., Hansen L.N. Evolution of the Josephine Peridotite Shear Zones: 2. Influences on Olivine CPO Evolution. *Journal of Geophysical Research: Solid Earth*. 2019. Vol. 124. Iss. 12, p. 12763-12781. DOI: 10.1029/2019JB017968

21. Soustelle V., Manthilake G. Deformation of olivine-orthopyroxene aggregates at high pressure and temperature: Implications for the seismic properties of the asthenosphere. *Tectonophysics*. 2017. Vol. 694, p. 385-399. DOI: 10.1016/j.tecto.2016.11.020

22. Michibayashi K., Mainprice D., Fujii A. et al. Natural olivine crystal-fabrics in the western Pacific convergence region: A new method to identify fabric type. *Earth and Planetary Science Letters*. 2016. Vol. 443, p. 70-80. DOI: 10.1016/j.epsl.2016.03.019

23. Munjae Park, Youngwoo Kil, Haemyeong Jung. Evolution of Deformation Fabrics Related to Petrogenesis of Upper Mantle Xenoliths Beneath the Baekdusan Volcano. *Minerals*. 2020. Vol. 10. Iss. 9. N 831. DOI: 10.3390/min10090831

24. Skemer P., Hansen L.N. Inferring upper-mantle flow from seismic anisotropy: An experimental perspective. *Tectonophysics*. 2016. Vol. 668-669, p. 1-14. DOI: 10.1016/j.tecto.2015.12.003

25. Saveliev D.E., Makatov D.K., Sergeev S.N. Microstructural features of chromitite and ultramafic rocks of Almaz-Zhemchuzhina deposit (Kempirsay massif, Kazakhstan). *Problemy mineralogii, petrografii i metallogenii. Nauchnye chteniya pamyati P.N.Chirvinskogo*. 2023. N 26, p. 230-235 (in Russian). DOI: 10.17072/chirvinsky.2023.230

26. Varyukhin V.N., Pashinskaya E.G., Zavdoveev A.V., Burkhovetskii V.V. Capabilities of the electron backscatter diffraction method for analysing the structure of deformed materials. Kiev: Naukova dumka, 2014, p. 104.

27. Adams B.L. Electron Backscatter Diffraction in Materials Science. Moscow: Tekhnosfera, 2014, p. 544.

28. Danilenko V.N., Mironov S.Y., Belyakov A.N., Zhilyaev A.P. Application of EBSD analysis of material physics (review). *Industrial Laboratory. Diagnostics of Materials.* 2012. Vol. 78. N 2, p. 28-46 (in Russian).

29. Savelyev A.A., Savelyeva G.N. The Kempersay massif ophiolites: main characteristics of the structure and substance evolution. *Geotectonics.* 1991. N 6, p. 57-75 (in Russian).

30. Balykin P.A., Konnikov E.G., Krivenko A.P. et al. Petrology of post-harzburgite intrusions of the Kempirsai-Khabarninskii ophiolite association (Southern Urals). Sverdlovsk: Institut geologii i geokhimii, 1991, p. 159 (in Russian).

31. Abdullin A.A., Avdeev A.V., Seitov N.S. Silurian ophiolites of the Sakmara and Or-Iletsk zones of the Mugodzhar. *Trudy Instituta geologicheskikh nauk KazSSR*. 1975, p. 39-74 (in Russian).

32. Saveliev D.E., Makatov D.K., Rakhimov I.R. et al. Silicates from Lherzolites in the South-Eastern Part of the Kempirsay Massif as the Source for Giant Chromitite Deposits (the Southern Urals, Kazakhstan). *Minerals*. 2022. Vol. 12. Iss. 8. N 1061. DOI: 10.3390/min12081061

33. Saveliev D.E., Makatov D.K., Vishnevskiy A.V., Gataullin R.A. Accessory Minerals in the Chromitite Ores of Dzharlybutak Ore Group of Kempirsai Massif (Southern Urals, Kazakhstan): Clues for Ore Genesis. *Minerals*. 2023. Vol. 13. Iss. 2. N 263. DOI: 10.3390/min13020263

34. Saveleva G.N., Pertsev A.N. Mantle ultramafic rocks in ophiolites of the Southern Urals, Kempirsai massif. *Petrologiya*. 1995. Vol. 3. N 2, p. 115-132 (in Russian).

35. Ballhaus C., Berry R.F., Green D.H. High pressure experimental calibration of the olivine-orthopyroxene-spinel oxygen geobarometer: implications for the oxidation state of the upper mantle. *Contributions to Mineralogy and Petrology*. 1991. Vol. 107. Iss. 1, p. 27-40. DOI: 10.1007/BF00311183

36. Ono A. Fe-Mg partitioning between spinel and olivine. *The Journal of the Japanese Association of Mineralogists, Petrologists and Economic Geologists*. 1983. Vol. 78. Iss. 4, p. 115-122. DOI: 10.2465/ganko1941.78.115

37. Roeder P.L., Campbell I.H., Jamieson H.E. A re-evaluation of the olivine-spinel geothermometer. *Contributions to Mineralogy and Petrology*. 1979. Vol. 68. Iss. 3, p. 325-334. DOI: 10.1007/BF00371554

38. Haemyeong Jung. Crystal preferred orientations of olivine, orthopyroxene, serpentine, chlorite, and amphibole, and implications for seismic anisotropy in subduction zones: a review. *Geosciences Journal*. 2017. Vol. 21. Iss. 6, p. 985-1011. DOI: 10.1007/s12303-017-0045-1

39. Yamamoto J., Ando J., Kagi H. et al. In situ strength measurements on natural upper-mantle minerals. *Physics and Chemistry of Minerals*. 2008. Vol. 35. Iss. 5, p. 249-257. DOI: 10.1007/s00269-008-0218-6

40. Saveliev D.E. Chromitites of the Kraka ophiolite (South Urals, Russia): geological, mineralogical and structural features. *Mineralium Deposita*. 2021. Vol. 56. Iss. 6, p. 1111-1132. DOI: 10.1007/s00126-021-01044-5

41. Saveliev D.E., Puchkov V.N., Sergeev S.N., Musabirov I.I. Deformation-induced decomposition of enstatite in mantle peridotite and its role in partial melting and chromite ore formation. *Doklady Earth Sciences.* 2017. Vol. 476. N 1, p. 1058-1061. DOI: 10.1134/S1028334X17090161

42. Ghosh B., Misra S., Morishita T. Plastic deformation and post-deformation annealing in chromite: Mechanisms and implications. *American Mineralogist*. 2017. Vol. 102. Iss. 1, p. 216-226. DOI: 10.2138/am-2017-5709

43. Johnson C. Podiform chromite at Voskhod, Kazakhstan: Submitted in partial fulfilment of the requirements for the degree of Ph.D. Cardiff University, 2012, p. 468.

44. White J.C., White S.H. On the structure of grain boundaries in tectonites. *Tectonophysics*. 1981. Vol. 78. Iss. 1-4, p. 613-628. DOI: 10.1016/0040-1951(81)90032-9

45. Spiess R., Peruzzo L., Prior D.J., Wheeler J. Development of garnet porphyroblasts by multiple nucleation, coalescence and boundary misorientation-driven rotations. *Journal of Metamorphic Geology*. 2001. Vol. 19. Iss. 3, p. 269-290. DOI: 10.1046/j.1525-1314.2001.00

***Authors*: Dmitrii E. Saveliev,** *Doctor of Geological and Mineralogical Sciences, Chief Researcher, savl71@mail.ru, https://orcid.org/0000-0001-8910-6992* (*Institute of Geology, Ufa Federal Research Centre of the RAS, Ufa, Russia*), **Semen N. Sergeev**, *Junior Researcher, https://orcid.org/0000-0001-5494-390X* (*Institute for Metals Superplasticity Problems of the RAS, Ufa, Russia*), **Darkhan K. Makatov**, *PhD Student, https://orcid.org/0009-0006-5059-2851* (*Abylkas Saginov Karaganda Technical University, Karaganda, Republic of Kazakhstan*).

The authors declare no conflict of interests.